THE JOURNAL OF PHYSICAL CHEMISTRY B

pubs.acs.org/JPCB Article

Ultrafast Fluorescence Signals from β-Dihydronicotinamide Adenine Dinucleotide: Resonant Energy Transfer in the Folded and Unfolded Forms

Andrea Cadena-Caicedo, Beatriz Gonzalez-Cano, Rafael López-Arteaga, Nuria Esturau-Escofet, and Jorge Peon*

Cite This: J. Phys. Chem. B 2020, 124, 519–530 Read Online

ABSTRACT: β-Dihydronicotinamide adenine dinucleotide (NADH) plays a critical role in biological redox processes. Inside the cell, NADH can be in a folded or an unfolded conformation, depending on the chemical environment that surrounds it. It is known that selective excitation of adenine in NADH can induce energy transfer events from this nucleotide to the reduced nicotinamide chromophore. From the anticipated time scales, this process must compete with adenine's internal conversion channel, which is known to occur in the sub-picosecond time scale. In this work, we studied the dynamics of the excited states of both chromophores in NADH through the time resolution of the spontaneous emission from both nucleotides. Through these experiments, we extend the knowledge about the competition between the different photophysical channels both in the folded and unfolded states. The study involved the folded and unfolded states of NADH by experiments in water and methanol solutions. Our femtosecond fluorescence results were complemented by the first nuclear magnetic resonance through space magnetization transfer measurements on NADH, which establish the solvent-dependent folded versus unfolded states. We determined the dynamics of the excited states by direct excitation of dihydronicotinamide at 380 nm and adenine at 266 nm. From this, we were able to measure for the folded state, a time constant of 90 fs for energy transfer. Additionally, we determined that even in what is referred to as an unfolded state in methanol, non-negligible excitation transfer events do take place. Spontaneous emission anisotropy measurements were used in order to confirm the presence of a minor energy transfer channel in the methanol solutions where the unfolded state dominates.

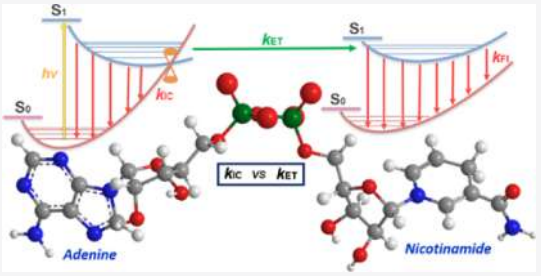

1. INTRODUCTION

β-Dihydronicotinamide adenine dinucleotide (NADH) is the principal electron donor for the electron transport chain of oxidative phosphorylation in the mitochondria, where it acts as a coenzyme in biological redox processes which result in adenosine 5′-triphosphate (ATP) generation.[1,2] NADH and reduced nicotinamide adenine dinucleotide phosphate are among the most important intrinsic cellular chromophores as they are highly fluorescent and absorb in the ultraviolet A region, with maximum absorption and emission wavelengths at 340 and 460 nm, respectively.[3] The majority of NADH's autofluorescence in living cells is observed in the mitochondria, where the concentration of this molecule is higher than in other cellular areas.[4,5] Several studies have investigated the importance of using intracellular NADH fluorescence as a biomarker of cell pathology.[6,7] For example, NADH's fluorescence intensity and redox ratio can be used to monitor mitochondrial dysfunction in vitro and in vivo.[8] In addition, the average fluorescence lifetime of NADH is related to oxygen consumption and to the level of ATP, which in turn is related to the relative rates for glycolysis to oxidative phosphorylation.[9,10] When NADH is bound to an enzyme, its spectroscopic properties change in comparison with the unbound state, exhibiting a fluorescence lifetime increment and up to a fourfold larger emission yield. These differences are related to NADH's molecular conformation and structural restrictions in the protein-bound state versus the free state.[11]

The molecular structure of NADH is composed of two nucleotides, adenine and reduced nicotinamide, which are joined by a pyrophosphate bridge. This structure causes NADH to have two conformations in solution, which correspond to a folded state and an unfolded state (see Scheme 1). The relative populations of these states depends on the polarity of the surrounding solvent, the pH, and the temperature.[2,12,13] In general, NADH can exist in an equilibrium between these two conformations as has been demonstrated by techniques such as nuclear magnetic resonance (NMR) and fluorescence spectroscopy.[2,12] These

Received: October 24, 2019
Revised: December 16, 2019
Published: December 26, 2019

https://dx.doi.org/10.1021/acs.jpcb.9b10012
J. Phys. Chem. B 2020, 124, 519–530

Scheme 1. Diagram of the Folded and Unfolded States of NADH

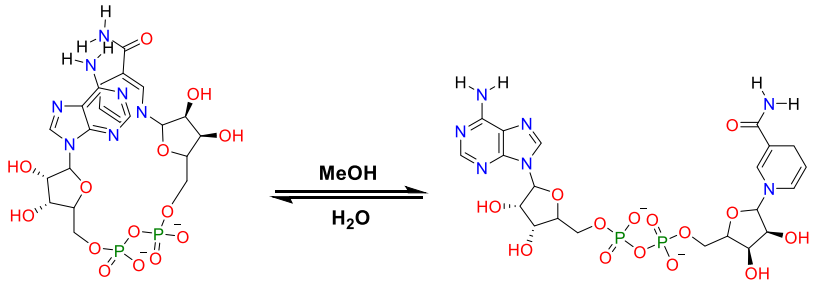

techniques have established that the population fraction in the folded state in aqueous solution is between 0.25 and 0.35.[14,15] In aqueous solution, NADH has an average fluorescence lifetime of approximately 0.4 ns. On the other hand, upon binding to enzymes like aldehyde dehydrogenase or malate dehydrogenase, NADH's conformation is considered to approach an unfolded or extended state.[16,17] Related to the binding and corresponding reduction in conformational variability, when NADH is bound to these proteins, its emissive state life time can reach up to 7 ns.[3,18] As mentioned, the variations in these properties are being used currently for the determination of different cellular metabolic states.[19]

Most of the NADH fluorescence studies rely on direct excitation of the reduced nicotinamide chromophore.[12,20,21] However, it is known that upon direct excitation of NADH's adenine chromophore, significant energy transfer can take place from this nucleotide to the nicotinamide heterocycle, resulting in an indirect excitation of this highly emissive fluorophore.[20] Previous spectroscopic studies have shown that the adenine to nicotinamide energy transfer yields depend on the folded state of NADH, given that resonant energy transfer is highly sensitive to the proximity of the donor−acceptor pair.[12,20,22]

The main focus of the present contribution is the study of the spontaneous emission signals from NADH in the sub-picosecond and picosecond time scales. Specifically, we describe the relaxation time scales upon excitation of each chromophore. Additionally, we follow the internucleotide energy transfer process through the femtosecond resolution of the fluorescence from both heterocycles. It is particularly interesting to understand the nature of these signals given that the adenine donor chromophore possesses one of the fastest internal conversion channels because of the presence of a directly accessed conical intersection between its first singlet excited state and its electronic ground state. Such surface crossing has been shown to produce S_1 decay rates with time constants of the order of 300 fs.[23,24]

Time-resolved spectroscopic studies of NADH have been performed only through transient absorption (TA) experiments.[22] In these studies, Heiner et al. observed excited state absorption signals associated to adenine and nicotinamide. These measurements assigned an ultrafast feature (sub-300-fs) to the decay of adenine's first singlet excited state because of internal conversion and energy migration to the nicotinic chromophore. Also, they found that energy migration forms a vibrationally hot first excited state of nicotinamide, which undergoes vibrational relaxation in a time scale of 1.7 ps. As in other studies, the TA measurements relied on the use of water/methanol mixtures to define the folded/unfolded state of NADH.[12,13,16]

The present fluorescence up-conversion study gives further details about the energy transfer process. In particular, the femtosecond resolution of the spontaneous emission allows for the full spectral isolation of the sub-picosecond signals associated to the population of the donor and acceptor excited states, without the need for spectral deconvolution. Also, the anisotropy of the signals provided by this technique allowed for an assessment of the relative angles of the transition dipole moments between adenine and dihydronicotinamide. For the objectives of our study, we include NMR-nuclear Overhauser enhancement spectroscopy (NOESY) measurements to evaluate the folded state population of NADH molecules in aqueous versus methanol solutions. Besides, we studied the time-resolved emission of the single chromophore analogs 1-benzyl-1,4-dihydrinicotinamide (NBz) and adenosine monophosphate (AMP) for crucial comparisons of the sub-picosecond spectral features of these single heterocycle systems with those of the NADH dinucleotide. We also include detailed excitation spectrum measurements in water/methanol mixtures, which reveal that even in what is considered the fully unfolded state, the adenine to nicotinamide energy transfer yield is non-negligible and corresponds to an important fraction of the nicotinic emission after excitation at 266 nm.

2. EXPERIMENTAL SECTION

2.1. Materials. The following substances were obtained from commercial sources: Nicotinamide adenine dinucleotide in the form of the reduced disodium salt hydrate-β-NADH (Sigma-Aldrich, ≥ 97%—HPLC grade), methanol (Sigma-Aldrich, HPLC Plus grade, ≥ 99.9%), potassium phosphate monobasic (Sigma-Aldrich, ACS reagent, ≥99%), sodium phosphate dibasic (Sigma-Aldrich, ACS reagent, ≥99%), and ultrapure deionized water (MILLIPORE Milli-Q system). 1-Benzyl-1,4-dihydronicotinamide−NBz (TCI Chemicals, HPLC grade, >95%). Phosphate buffer solutions (0.02 M) were prepared by dissolving an appropriate amount of dibasic sodium phosphate and monobasic potassium phosphate. The pH was adjusted to 7.4, using a 0.01 M NaOH solution. The NADH solutions (2×10^{-3} M) in aqueous phosphate buffer, methanol, and water/methanol mixtures were prepared freshly before each measurement. The water/methanol mixtures were prepared with a range of 0−100% of methanol. Concentrations of methanol were determined using the reported density of 0.7914 g/mL.[25]

2.2. Methods and Instrumentation. *2.2.1. Steady-State Spectroscopy.* Absorption and fluorescence spectra were measured in a Cary-50 (Varian) spectrophotometer and a Cary Eclipse (Varian) fluorimeter, respectively. All spectra were taken at room temperature (20 ± 1 °C) in a 1 cm-pathlength quartz cell.

https://dx.doi.org/10.1021/acs.jpcb.9b10012
J. Phys. Chem. B 2020, 124, 519−530

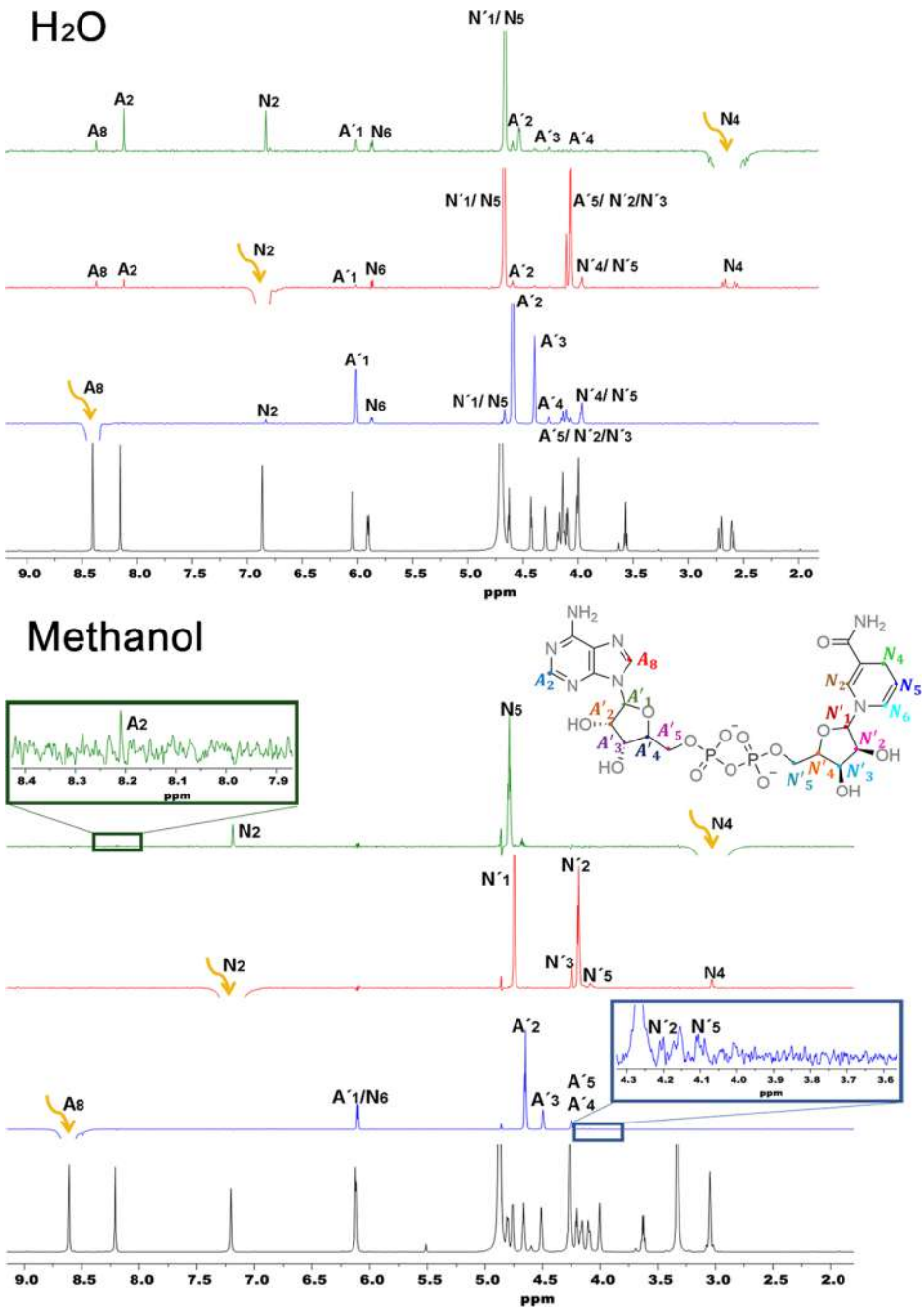

Figure 1. Selective 1D NOESY and ^{1}H NMR spectra (700 MHz, 298 K) of NADH in deuterated aqueous and methanol solutions. From top to bottom in each solvent: Selective inversion of protons N_4, N_2, and A_8 (indicated by arrows), and conventional ^{1}H spectrum (black line). The detailed NMR data and assignments are included in the Supporting Information.

2.2.2. Femtosecond Up-Conversion Measurements. The femtosecond up-conversion measurements were used to follow the ultrafast relaxation processes in the folded and unfolded conformations of NADH. Our setup has been reported previously.[26,27] Briefly, a Ti:Sapphire oscillator was pumped by a Nd:YLF laser (527 nm, 5 W) to obtain ultrashort pulses that are subsequently amplified by a regenerative amplifier (760 or 800 nm, 1 KHz, 100 fs, 620 mW). After amplification, the beam was divided using appropriate beam splitters. A first beam splitter directed the beam (gate pulses) to a delay stage and focused onto a nonlinear β-BBO crystal. The second beam (pump pulses) was used to generate the second harmonic (380 nm) by means of another β-BBO crystal. The third harmonic (266 nm after tuning the fundamental to 800 nm, using the 400 nm harmonic) was generated using another fraction of the beam from an additional beam splitter; this portion of the fundamental was mixed with the second harmonic in another β-BBO crystal. The polarization of the pump beam was set to the magic angle (54.7°) with respect to probe beam polarization (vertical), which coincided with the optical acceptance axis of the up-conversion β-BBO crystal. With this setup, the phase matching angle for the up-conversion process is adjusted through rotations of the crystal in the horizontal plane. The third harmonic or the second harmonic beams were focused into a fast-flow 1 mm quartz cell, where the NADH solutions were kept flowing continuously. The

https://dx.doi.org/10.1021/acs.jpcb.9b10012
J. Phys. Chem. B 2020, 124, 519−530

fluorescence generated by the pump beam was collected and focused by two parabolic mirrors. Residual excitation from the probe beam was eliminated by a long-pass optical filter for the second harmonic experiments or a UV band pass for the third harmonic experiments. The fluorescence and probe beams were then focused into the up-conversion nonlinear β-BBO crystal and the crystal phase matching angle was adjusted to obtain the respective sum frequency mixing signal with horizontal polarization (Scheme S1). This signal was finally directed to a double monochromator and detected with a photomultiplier tube. The NADH signal was resolved for emission wavelengths from 310 to 370 nm and from 440 to 620 nm with 10 nm steps. The instrument response function was determined to be Gaussian with a full width at half-maximum between 300 and 450 fs through the deconvoluted fluorescence traces of Coumarin 153 in methanol solution.[26] Finally, time-resolved fluorescence anisotropies (eq 1) were determined after adjusting the polarization of the pump beam with an appropriate wave plate to measure the perpendicular ($I_\perp$) and parallel ($I_\parallel$) components of the spontaneous emission intensities. The parallel and perpendicular fluorescence intensities were recorded sequentially with individual measurements (HH−VVVV−HH, where H and V stand for perpendicular and parallel emission intensities with respect to the excitation polarization axis). Finally, the geometrical factor (G) was within 4% of unity (determined using the long-lived emission of Coumarin 153).

$$r(t) = \frac{I_\parallel - I_\perp}{I_\parallel + 2I_\perp} \quad (1)$$

2.2.3. NMR Spectroscopy Measurements. ^{1}NMR spectra were recorded at 298 K on a Bruker 700 MHz AVANCE III HD NMR spectrometer, equipped with a (H-C/N-D) cryoprobe. For each experiment, fresh samples were prepared in 5 mm tubes where approximately 0.7 mL of 10 mM NADH was taken in the form of deuterated aqueous or methanol solutions, respectively.

The ^{1}H NMR spectra were acquired using the Bruker pulse sequences zg30 with an acquisition time of 2.3 s and 16 scans. The selective 1D NOESY experiments were collected using the Bruker pulse sequence *selnogpzs*, which minimizes artifacts in NOESY spectra arising from the evolution of zero-quantum contributions from scalar-coupled protons during the mixing time.[28] The experiments were recorded with a mixing time of 800 ms, an acquisition time of 2.3 s, and 4096 scans. Finally, the data were processed in the MestReNova 8.1 program and apodized with exponential functions of 1.5 Hz.

3. RESULTS AND DISCUSSION

3.1. NMR Spectroscopy in Aqueous and Methanol Solutions. Figure 1 shows a series of selective 1D NOESY (nuclear Overhauser effect spectroscopy) measurements of deuterated aqueous and methanol solutions of NADH. These are the first experiments which detect through space magnetization transfer signals between the two chromophoric units of NADH. NOESY experiments are used to quantify nuclear Overhauser effects, which are observed between protons that are close in space (i.e., separated by <5 Å). Several NOESY signals were detected for the NADH solutions. The proton NMR spectra and proton assignments of NADH are included in Figures S1 and S2 and Table S1 of the Supporting Information. From this assignment, the NOESY signals that are present upon selective excitation of several protons are summarized in Table S2.

For the aqueous solution, the NOE correlations associated with the irradiation of adenine's A8 and with dihydronicotinamide's N2 and N4 protons are a signature of the population of molecules in the folded conformation in water. Additionally, there are NOESY signals associated to the coupling of the adeninic protons to the ribose unit bound to nicotinamide. In congruence, upon irradiation of the nicotinamidic protons N2 and N4, the respective NOE to the adenines A8 and A2 are observed. Other NOE couplings are observed as illustrated in Figure 1. It can be noticed that a larger magnetization transfer is observed between N_4 and A_2, from which it can be concluded that the six-membered cycle of adenine may be tilted toward the reduced nicotinamidic fragment in the folded conformers, in a way that these two atoms are in close proximity.

For the methanolic solutions, excitation of the A8 proton again produces correlations with the ribose protons directly bound to the adenine system (the signals associated to the pair A′1 and N6 are observed because of their spectral proximity). In addition, very weak NOE correlations are detected with N_2' and N_5' (ribose protons bound to nicotinamide). These signals are only slightly above the noise level. Congruently, the selective inversion of the dihydronicotinamide proton N4 shows a very weak NOE correlation signal with adenine's A_2 proton. The presence of these NOE's correlations implies that the population of NADH molecules in methanol in which the two chromophores remain within a 5 Å distance is small but non-negligible. The NOESY intensity for the N_2 proton upon N_4 irradiation can serve to quantify this population. Specifically, the N_2 intensity in each solution can be used as a scale because of its inter-ring proximity to N_4, which makes this NOESY signal insensitive to the unfolding conformational changes. The A_2/N_2 NOE intensity ratio upon N_4 excitation in methanol is approximately a 4% fraction of its value in water. The non-negligible interaction between the N_4 and A_2 protons in methanol implies that even in methanol, there is a small fraction of the population where the adenine and nicotinamide systems can interact through magnetization or energy transfer. As we show below, this is consistent with our UV excitation experiments and the time-resolved emission measurements.

3.2. Steady-State Spectroscopy. The absorption, emission, and excitation spectra of NADH in water and methanol are presented in Figure 2. The absorption spectrum shows maxima at 260 and 340 nm. This spectrum can be decomposed into the contributions from adenine and reduced

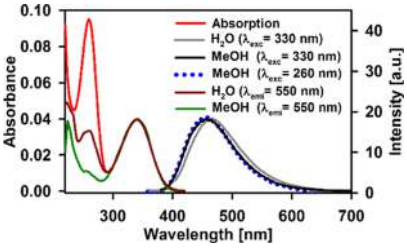

Figure 2. Absorption, emission, and excitation (detection: 550 nm) spectra of NADH solutions. The emission spectra in aqueous solution are shown in gray, and for methanol (MeOH) in black (excitation: 330 nm) and blue symbols (excitation: 260 nm). The excitation spectrum in aqueous solution is shown in purple and in methanol in green.

https://dx.doi.org/10.1021/acs.jpcb.9b10012
J. Phys. Chem. B 2020, 124, 519−530

nicotinamide.[12,29,30] The absorption at the longer wavelength band is solely due to dihydronicotinamide. For the shorter wavelength absorption band centered at 260 nm, the absorbance is mainly but not only from the adenosine chromophore (see below). For the single emission band, there is a small difference between the methanol and water emission spectra. In methanol, the spectrum has a maximum at 456 nm, whereas the aqueous solution spectrum presents a bathochromic shift to 466 nm. Upon the direct excitation of dihydronicotinamide (λ_{exc} = 330 nm), the fluorescence yields are 0.025 and 0.018 in aqueous and methanol solutions respectively. These results were obtained using Coumarin 102 in ethanol as a standard solution (fluorescence yield: 0.80, λ_{exc} = 390 nm, λ_{emi} = 466 nm).[31] The respective net emission yields of NADH upon 260 nm excitation were 0.008 in water and 0.003 in methanol.

The excitation spectra of NADH are included for both solvents in Figure 2. As can be seen, upon scaling the long wavelength excitation band to NADH's absorption spectrum, the shorter wavelength band (near 260 nm) corresponds to a significantly smaller intensity in comparison with the absorption peak at this wavelength. Also, the intensity in the excitation spectrum at 260 nm is different for the aqueous solution in comparison with the methanolic one.

In order to determine the precise relative contributions to the absorption in the region around the 260 nm band, we also studied the steady-state spectra of the analog-reduced nicotinamide system NBz (see Scheme 2). The respective absorption spectrum is included in the inset of Figure 3. The NBz molecule has the same substitution pattern for the 1,4-dihydronicotinamide chromophore but without the pyrophosphate bridge and the adeninic section. The spectra of NBz were taken in methanol. Because of a small amount of solvatochromism, for the comparisons with the NADH solutions, the acquired NBz spectrum was shifted by 12 nm so that the long wavelength band perfectly matches the NADH spectra in water and methanol. From the comparison with NBz, the absorption at the 260 nm band of NADH corresponds to 94%, and the rest is related to residual absorption by the dihydronicotinamidic system.

Scheme 2. Structure of NBz

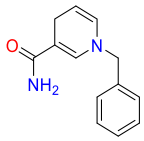

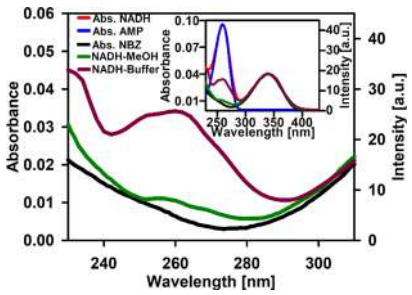

Figure 3. Absorption spectrum of the nicotinamidic analog NBz (black line), and excitation spectra of NADH (detection: 550 nm) in water (purple line) and methanol (green line) in the region of adenine's first absorption band. The absorption spectra of NADH and AMP in water are included additionally in the inset (red line and blue line, respectively). The NBz absorption spectrum was taken in methanol solution and was shifted by 12 nm in order to match the 340 nm absorption band of NADH. In the Supporting Information, we show that the excitation spectra of these samples is independent of the detection wavelength in the region of dihydronicotinamide emission.

As mentioned in previous reports,[12,16,20−22] considering that NADH's short wavelength band has a prominent contribution from the adenine absorbance, the existence of significant nicotinamidic emission upon excitation in the 240 to 280 nm region is indicative of adenine to nicotinamide energy transfer. The excitation spectra in aqueous and methanolic solutions can be used to quantify the yield for adenine to dihydronicotinamide energy migration. Although this kind of analysis has been performed previously,[12,22] such studies did not take into account the spectral decomposition which we perform herein using the NBz absorption spectrum. The intensity of the excitation peak at 260 nm is a measure of the energy transfer yield in both solutions. In water, this excitation feature has been associated previously to the folded state.[12,22] With respect to the NADH/methanol sample, the excitation spectrum we present in Figures 2 and 3 shows a small but clear peak around 260 nm (above the scaled absorption of NBz used to quantify the intensity because of residual dihydronicotinamide absorption and that from adenine absorption). This feature is highlighted in the main section of Figure 3. This small peak is highly reproducible and has been observed in previous studies,[12] but was overseen in another one.[22] This feature implies a small but relevant (see below) amount of adenine to nicotinamide energy transfer in the methanolic solution.

The energy transfer yields in water and methanol solutions were calculated according to

$$\varphi_{ET} = \frac{I_{260}^{ade}}{A_{260}} \frac{A_{340}}{I_{340}}$$

where the transfer yield φ_{ET} depends on I_{260}^{ade}, which is the 480 nm detected intensity for 260 nm excitation because of adeninic-only absorbance (i.e., after subtraction of the intensity associated to direct dihydronicotinamidic excitation at 260 nm). A_{260} is NADH's absorbance at this wavelength, and A_{340}/I_{340} is the normalization factor (where I_λ is the fluorescence intensity at the respective wavelength). The energy transfer yield that can be calculated from the excitation spectra corresponds to 0.3 in aqueous solution and to 0.05 for the methanolic solutions. Importantly, from the excitation spectra, the NADH emission upon excitation at 260 nm which is due to adenine excitation, corresponds to 82% in water and 43% in methanol, where the rest is due to the residual absorption of the dihydronicotinamide band considering NBz as a proxy for the absorption of this heterocycle at 260 nm. This result implies that the energy transfer after adeninic absorption in NADH/methanol is significant (0.05), and consistent with the fact that the NOESY signals described in the previous section show a relative amplitude of $1/(0.04 \pm 0.015)$ for NADH's aqueous versus methanolic solutions.

The steady-state emission characteristics of water/methanol mixtures are described next. As can be seen in Figure S3, increasing the methanol mole fraction of the mixture causes a decrease in the intensity of the excitation band at 260 nm. As

https://dx.doi.org/10.1021/acs.jpcb.9b10012
J. Phys. Chem. B 2020, 124, 519−530

mentioned previously, this is related to an increase in the population of the unfolded conformation of the NADH for the larger methanol fractions and the respective reduction in the energy transfer yield.[12,16,22] These results will be used as the basis for the explanation of the femtosecond resolved emission traces (see below).

For our objectives, it was important to study the spectral features of AMP in order to directly compare them against the NADH dinucleotide. Figure 4 shows the steady-state

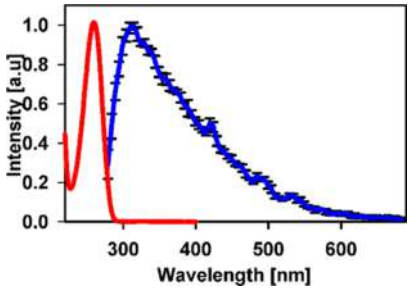

Figure 4. Steady-state absorption (red) and emission (blue) spectra of AMP in aqueous solution.

absorption and emission spectra from an AMP aqueous solution. The emission spectrum of AMP shows a broad band from 310 to 620 nm. Such a broad and faint emission spectrum in AMP is related directly to its highly efficient S_1 to S_0 internal conversion because of the presence of a directly accessed conical intersection, which redounds in an approximately 300 fs fluorescent state lifetime.[24,29,32] Specifically, the fluorescence from AMP is produced only within the first picosecond after excitation, where the emission transitions take place while the system is evolving along a path in the potential energy surface where the S_1 and S_0 surfaces approach each other.[23,33] Such reduction in the intersurface gap in the time scale in which the emission is produced (as the system reaches the S_1 to S_0 conical intersection) causes a broad distribution of photon energies. The fluorescence quantum yield in AMP was estimated to be 1×10^{-5} using *p*-terphenyl as a standard (fluorescence quantum yield: 0.93). This quantum yield of AMP is consistent with previous reports.[22,32] The characterization of the faint steady-state emission from adenine in AMP will be of crucial value for the understanding of NADH's time-resolved signals.

3.3. Femtosecond-Resolved Emission of NADH with Direct Excitation of Nicotinamide at 380 nm. Although NADH is one of the most important fluorescent molecules in biological systems, this is the first characterization of its early (sub-picosecond and picosecond) emission dynamics. Typical traces in aqueous buffered solution and in methanol are presented in Figure 5 for direct 380 nm excitation. The deconvoluted time-resolved spectra are also included.

As can be seen, the up-conversion signals show an instrument-limited rise as a function of pump-gate delay time, reflecting the direct formation of the emissive state. In both solvents, there are also small amplitude decays on the shorter-wavelength region of the spectrum, and rises on the longer-wavelength side, all occurring with time constants of several picoseconds (see Tables S3 and S4) These signal rises and decays on each side of the spectrum, and the respective spectral shift, are characteristic of relaxation processes (typically from solvation), which produce a decrease in the

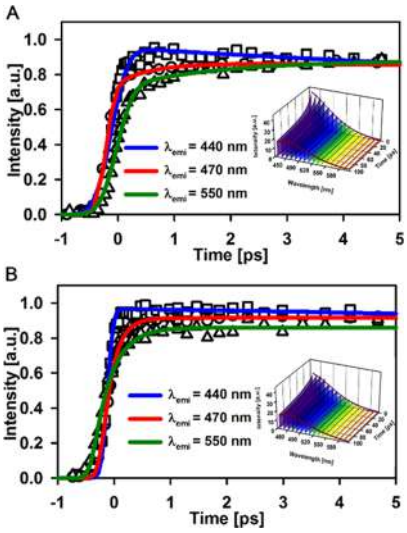

Figure 5. Time-resolved emission traces and deconvoluted spectra of NADH in (A) aqueous and (B) methanol solutions after direct nicotinamide excitation at 380 nm. The wavelength-dependent time-resolved fluorescence spectra were reconstructed from the convoluted fits to the up-conversion traces.

energy gap between the emissive state and the ground state. Such features are followed by a single exponential decay of 284 ± 6 ps in water and 330 ± 12 ps in methanol. These time constants correspond to the S_1 lifetimes of NADH, excited in the dihydronicotinamide chromophore.[3,17,18,34] The picosecond features imply that, in both solvents, the spectral maxima undergoes a red shift in the time scale of several picoseconds. In the case of methanol, the time scales of the spectral shift and the decays on the red side are typical of relaxation processes which produce a dynamical Stokes shift in this solvent (see Table S4).[35]

For the aqueous solutions of NADH, the blue side decays, the red side rises, and concomitant red-shifting of the spectra take place on time scales that cannot be attributed only to solvent relaxation. Water is one of the solvents with the fastest relaxation times, where the respective dynamical Stokes shift occurs with time constants that go from the sub-100-fs time scale up to 1 ps.[36] From the data in Figure 5, the dynamical Stokes shift observed for NADH in water is significantly slower, and the time constants associated with the red shift go from 2 to 46 ps (see Table S3). Accordingly, it is reasonable to suggest that the spectral shift of NADH is related to the relaxation of the folded conformation which has been established as having contacts between the adenine and nicotinamide heterocycles. Therefore, the aqueous "solvation shell" of the nicotinamide fluorophore is expected to be replaced partially by the rest of the NADH system. With this consideration, it would be expected that different relaxation (and red shift) times exist from the ones that would be observed if the fluorophore was fully solvated. As mentioned, although the dihydronicotinamidic heterocycle is one of the most studied chromophores in biochemistry, this is the first detailed description of its dynamics in the picosecond time scale.

3.4. Time-Resolved Spectra of the Ultrafast S_1 Decay of AMP. In order to establish the contributions of both chromophores to the time-resolved spontaneous emission signals across the spectrum of NADH, we required a detailed understanding of the time-resolved signals because of adenine

https://dx.doi.org/10.1021/acs.jpcb.9b10012
J. Phys. Chem. B 2020, 124, 519−530

emission. For this, we used the AMP molecule as a reference system. The spectral evolution after 266 nm excitation in AMP is included in Figure 6. As can be seen, for all the wavelengths

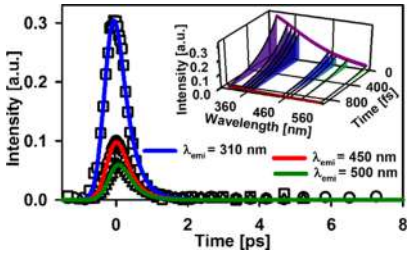

Figure 6. Time-resolved emission spectra of AMP in aqueous solution after 266 nm excitation. The inset shows the respective reconstructed deconvoluted time-resolved decays at several wavelengths. Some spectral zones do not show traces as in these regions the up-conversion measurements cannot be performed because of interactions in the sum frequency mixing optical crystal.

of the broad emission spectrum of this molecule, we observe sub-picosecond decays. Although several studies have been made about the ultrafast decay of the emissive state of adenine, adenosine, or AMP, the full time-resolved spectral evolution had not been reconstructed.[24,32,37] Adenine is well known for its ultrafast S_1 to S_0 internal conversion. This efficient process is mediated by a conical intersection, which is accessed directly after vertical excitation.[24,29,32] Notably, these signals are more intense at wavelengths below the spectral zone of the emission of dihydronicotinamide (400 to 600 nm); however, the time-gated emission can still be clearly detected within this spectral region and above. In fact, the sub-500-fs features can be observed up to 560 nm, more than 2.5 eV from the first absorption band. The time constants for these decays only show minor changes across the spectrum.[37] The details of the time-resolved adenosine emission will be relevant for the discussions of the sub-picosecond features of the emission of NADH after adenine excitation at 266 nm (see below).

3.5. Time-Resolved Emission of NADH after 266 nm Excitation. Figures 7−10 show the up-conversion results for NADH in aqueous and methanol solutions for 266 nm excitation. From the previous discussion, the emission from the locally excited adeninic chromophore is the only contribution to the transient signals in the region from 320 to 360 nm. Above this region, both chromophores contribute to the time-resolved signals. In the first region, the traces are very similar to those observed in the AMP solutions where the emission decays to the baseline with time constant of less than 300 fs for both water and methanol. We will return to the description of these signals in a paragraph below. On the other hand, in the region above 400 nm, the water and methanol solutions show drastic differences.

For the aqueous NADH solutions in the region above 400 nm, the water solutions show an ultrafast rise of less than 300 fs (see Figure 8A). This signal rise corresponds to an exponential term with negative coefficient where the time constant is such that it can be distinguished from an instantaneous signal. However, from the uncertainty in the time constant parameter, only its upper bound value can be established. The sub-300-fs signal increment is followed by small-amplitude rises (below 520 nm) or decays (above 530 nm) with time constants of several picoseconds (all time constants are included in the Supporting Information in Table

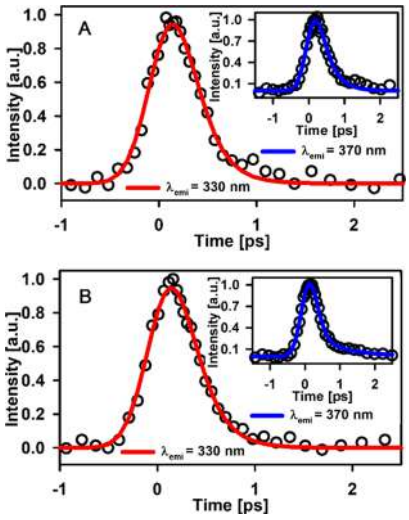

Figure 7. Typical up-conversion traces at representative wavelengths for NADH excited with 266 nm pulses in (A) aqueous and (B) methanol solution for the spectral region where only the adenine emissions are observed.

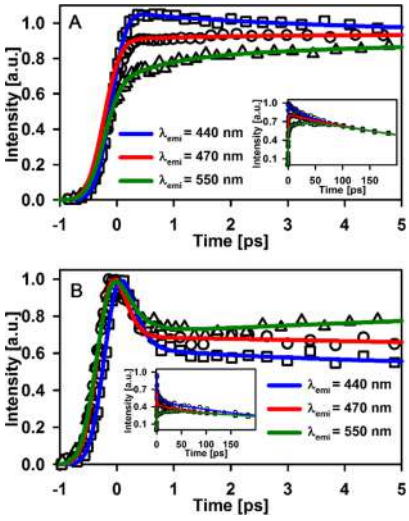

Figure 8. Typical up-conversion traces at representative wavelengths for NADH excited with 266 nm pulses in (A) aqueous and (B) methanol solution. Detection wavelengths correspond to the 440 to 600 nm region, which corresponds to the dihydronicotinamide chromophore emission band.

S5). The intermediate rises or decays are followed by the fluorescence decay times, which match NADH's excited-state lifetime (447 ps in water). Considering the ultrafast decay of the adeninic excited state, and because of the proximity of the two chromophores in the folded state, the signal rises of less than 300 fs were interpreted to be due mostly to energy transfer from adenine's short-lived first singled excited state.

For the NADH/methanol solutions with 266 nm excitation in the region above 400 nm (see Figure 8B), the early features are significantly different from those in water. Specifically, instead of a sub-300-fs signal rise, the signals can be described by an instantaneous signal appearance, followed by a sub-300-fs decay across the spectral region. This rapid decay settles to an amplitude level where similar picosecond time constants are observed as in the case of water (Table S6). This intermediate time scale of several picoseconds and the fluorescence lifetime

https://dx.doi.org/10.1021/acs.jpcb.9b10012
J. Phys. Chem. B 2020, 124, 519−530

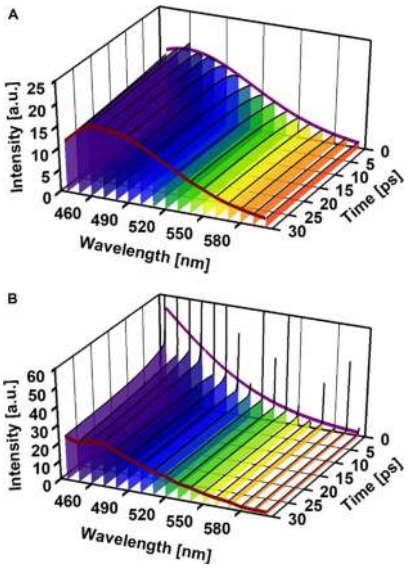

Figure 9. Time-resolved emission spectra of NADH in (A) aqueous and (B) methanol solutions after 266 nm excitation.

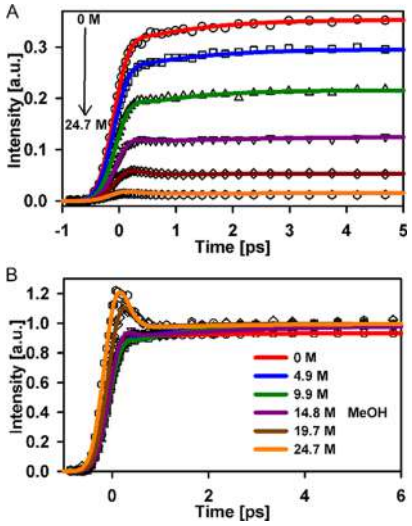

Figure 10. Fluorescence up-conversion transients of NADH in different water/methanol mixtures λ_{exc} = 266 nm and λ_{emi} = 470 nm (A). In the lower graph (B), the signals were scaled in order to emphasize the differences in the signal features near t = 0.

are (as expected) not altered significantly in comparison with the corresponding experiments with 380 nm excitation.

Given the previous description of the signals from the AMP experiments and the NADH experiments with 380 nm excitation, the interpretation of the differences between aqueous and methanol solutions for 266 nm excitation is as follows: In the region below 370 nm, the up-conversion experiments isolate the spontaneous emission of the adenine chromophore, which is locally excited with the 266 nm pulses. This decay is ultrafast and because of the net depopulation of the adenine S_1 state, where the total population decay rate is due to more than one channel and now includes energy transfer to the dihydronicotinamide moiety (see below).

Considering the steady-state NADH emission and the broad emission seen in AMP for the region above 370 nm, the time-resolved emission (Figure 9) must correspond to both chromophores (adenine and dihydronicotinamide) where the energy transfer channel produces an accumulation of the nicotinamide-excited population. In the case of NADH in aqueous solutions, the net effect corresponds to an ultrafast accumulation of the nicotinamide-excited population (hence the sub-300-fs rise). For the NADH/methanol case, the unfolded population and concomitant interchromophore distance implies a much-diminished efficiency for energy transfer. The net emission in this region for the methanol solutions then see an overlap of the emission decay from the adeninic chromophore, and the accumulation and much slower relaxation and decay of the nicotinamidic fluorescent state. That is, the ultrafast decay corresponds to the loss of the adenine S_1 population, which leaves a signal offset (or near plateau) associated to the transient emission from nicotinamide.

The previous interpretation can be supported further by a series of experiments in which the methanol content is increased gradually. The results are included in Figure 10, which shows up-conversion traces of NADH with detection at 470 nm (dihydronicotinamide emission) after adenine excitation. As can be seen, through the increase of the methanol concentration, the gradual signal rise in the buffered aqueous solutions (exponential rise of approximately 300 fs) is gradually converted into an instrument-limited signal followed by an ultrafast decay of less than 300 fs. As can be seen, this kind of transient can be used to ascertain the folding state of the NADH molecule in the context of the biochemical environment. As expected, the dihydronicotinamide fluorescent state lifetime shifts from 447 ps in water to 325 ps in methanol. The fit parameters for the decays are included in Table S7.

For 266 nm excitation, a detailed inspection of the NADH signals in the sub-400-nm region reveals small differences between the AMP, NADH/methanol, and NADH/water solutions (see Figure 11).

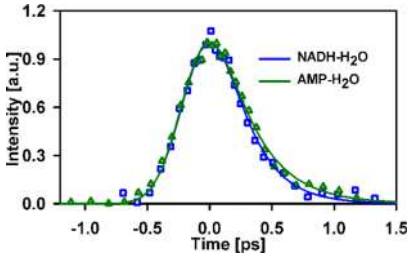

Figure 11. Femtosecond fluorescence up-conversion traces of AMP (green) and NADH (blue) in aqueous solution. The excitation wavelength was 266 nm and the detection wavelength was 350 nm.

The time-resolved signals in the spectral region where only the adeninic chromophore contributes can produce a direct estimate of the energy transfer rate. Given that the decay time of the emission of AMP reflects the rate of decay of the S_1 state of the adenine chromophore because of the internal conversion channel, the changes in the observed S_1 decay times can be directly assigned to the presence of the additional energy transfer channel in NADH without the requirement for any spectral deconvolution. As can be seen in Figure 11, the spontaneous emission signal at 350 nm (region of adenine-only emission) decays in a somewhat faster time scale. Importantly, the two traces in Figure 11 were taken in a back-to-back fashion and under identical alignment conditions. The AMP

https://dx.doi.org/10.1021/acs.jpcb.9b10012
J. Phys. Chem. B 2020, 124, 519−530

solution shows an up-conversion signal, which was fitted to a single exponential decay convoluted with a Gaussian instrument response time. The time constant for the decay in this case was of 300 ± 50 fs, which is in excellent agreement with the most recent measurements of AMP and adenosine for the same excitation wavelength.[37] On the other hand, the signals for the NADH/water solutions show a shorter decay time of 230 ± 50 fs. Also, it was verified that from visual inspection of both fits that the two experiments have apparently different exponential decay functions (see Figure 11). The respective traces for NADH in methanol show a decay time of 275 ± 50 fs. Considering that the NADH molecules in aqueous solution have approximately a 30% population fraction in the folded state,[14,15] the 230 fs adeninic S_1 state water should be taken as an average lifetime of both kinds of conformers (with sufficient time resolution, it might be possible to distinguish the two time scales as a biexponential decay; however, because of our limited time resolution, the observed lifetime can only be taken as an average value). From the 70/30 relative unfolded/folded population fractions, and considering that the unfolded population should retain a similar 300 fs lifetime, the excited-state lifetime for the folded population can be estimated to be of 67 fs (considering a simple average pondered by the 0.7 and 0.3 fractions of the NADH populations, these fractions were taken as the average of the reported unfolded/folded from emission, NMR,[14,15,38] and TA measurements).[22] From the total decay rate of the adeninic excited state for the folded population ($k_{total,folded} = (67\ fs)^{-1}$), and taking the internal conversion rate to be $k_{IC} = (300\ fs)^{-1}$, the energy transfer rate can be determined from $k_{total,folded} = k_{IC} + k_{ET,folded}$ to be $k_{ET,folded} \approx 1.16 \times 10^{13}\ s^{-1}$ with an uncertainty of the order of 50% from a simple error propagation scheme associated to the errors in the respective up-conversion lifetimes of Figure 11. The value of $k_{ET,folded}$ compares very well with a previous value of $1.5 \pm 1.4 \times 10^{13}\ s^{-1}$ from a TA measurement in aqueous solution.[22]

3.6. Fluorescence Anisotropy Measurements. To study the femtosecond evolution of the relative orientation of excitation and emission transition dipole moments during the different photophysical processes, we measured the fluorescence anisotropy and determined the β angle (formed by the dipole moments of absorption and emission) of NADH in aqueous and methanol solutions after excitation with 266 and 380 nm. We also studied the anisotropy of the emission of the reference molecule NBz with both excitation wavelengths. The results are shown in Figures 12, S4, and S5.

Upon 380 nm excitation of NADH, the fluorescence anisotropy measurements near $t = 0$ (r_0) show a value consistent with nearly parallel absorption and emission transitions (~0.3).[3,39,40] The anisotropy decays indicate rotational diffusion times of the nicotinamide-excited molecules and correspond to 133 ± 2 and 153 ± 3 ps in water and methanol, respectively. With these results, NADH's hydrodynamic volumes in each solvent were estimated using a simple Debye–Stokes–Einstein model: $\theta = \eta V/kT$, where θ is the anisotropy decay time, η is the viscosity (0.958 cP for water and 0.533 cP for methanol), V is the molecular hydrodynamic volume, T is the temperature in Kelvin (298 K), and k the Boltzmann constant. The resulting hydrodynamic volumes correspond to 570 ± 10 Å^3 in water and 1180 ± 10 Å^3. The hydrodynamic volume in water compares very well with a previous time-correlated single photon counting (TCSPC) measurement of 544 Å^3.[40] It should be noted that these are

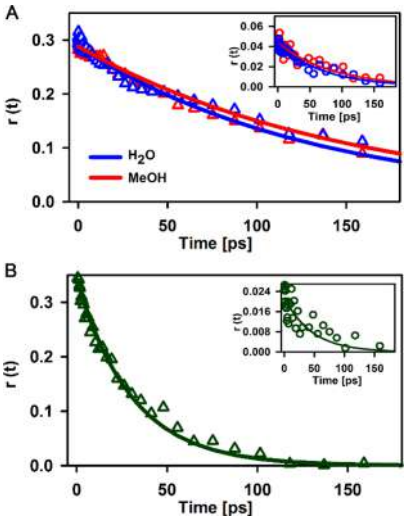

Figure 12. Fluorescence anisotropy detected at 470 nm exciting at 380 and 266 nm (inset). NADH in aqueous and methanol solution (A) and NBz in methanol solution (B).

simple estimated average numbers as, in particular in water, there are different kinds of conformations (folded and unfolded). The smaller (average) hydrodynamic volume in water therefore can be directly associated to the folded subpopulation, which can be expected to have a smaller hydrodynamic volume. The $t = 0$ anisotropy value is below the ideal 0.4 value for parallel excitation and emission transition dipole moments, and comparable to a value reported previously.[40]

The insets of Figure 12 also show the fluorescence anisotropy traces detected at 470 nm after 266 nm excitation. This corresponds to nicotinamide emission after excitation in the region of the adenine absorption. The initial anisotropies of NADH in aqueous and methanol solutions have values of 0.04 ± 0.01 ($\beta = 50.8°$) and 0.045 ± 0.01 ($\beta = 50.2°$), respectively, where β is the angle between the excitation transition dipole moment and that of the emission. The time-resolved anisotropy traces show decays to the base line with the same time constants as in the case of 380 nm excitation. For 266 nm excitation, the r_0 values are quite small and also similar in both solutions. In these experiments, r_0 is defined by the relative orientation of the transition dipole moments of the adenine absorption transition and the nicotinamide emission because of the energy transfer coupling, and also, from a contribution of the relative orientation between the adeninic absorption transition dipole at 266 nm (a higher singlet state, see below), and the emission transition moment of nicotinamide's S_1 state.

For 266 nm excitation of the reference molecule NBz, r_0 has an even smaller anisotropy value of 0.02, which corresponds to a β value of 52.7°. For this molecule, the r_0 value is set only by the relative orientation of the 266 nm transition dipole moment (most likely to a superposition of higher singlet states of NBz) and that of its $S_1 \rightarrow S_0$ emissive state, which is formed by internal conversion. As we described above, the NADH/methanol and the NADH/water solutions show a twofold higher value of r_0. This difference is consistent with the presence of the energy transfer channel for NADH/water, and also is indicative of a contribution of the energy transfer channel for the NADH/methanol system. That is, the 440 nm emission after 266 nm excitation in these solutions is in part

https://dx.doi.org/10.1021/acs.jpcb.9b10012
J. Phys. Chem. B 2020, 124, 519–530

because of direct excitation of the dihydronicotinamide higher states and in part because of adenine excitation. In summary, from the excitation spectra, the contribution to the diyhydronicotinamidic emission from adeninic absorption is 82% in water and 43% in methanol; if the direct nicotinamidic excitation at 266 nm was the only channel for 440 nm emission in NADH/methanol, it would be expected that the r_0 value would be the same as that in the NBz system. The observed anisotropy value in methanol after adenine excitation is consistent with a significant portion of the emission of 43% arising from the energy transfer channel.

3.7. Estimate of the Average Donor−Acceptor Distance in Methanol. From the observed lifetime of NADH's adeninic emission in methanol, it is possible to estimate the average rate constant for energy transfer in this solvent. Given the 275 fs decay, and comparing this value with the internal conversion time for adenine (300 fs), and with the expression for the total decay constant of adenine's S_1 state, ($k_{total} = k_{IC} + k_{ET}$), we estimate the transfer rate constant to be $k_{ET} \approx 3 \times 10^{11}$ s^{-1}. From this value, it was possible to determine an average adenine-nicotinamide distance in methanol considering Förster's relation for the rate constant as a function of the donor−acceptor distance.[3,41] Using the well-known Föster formula with an orientation factor $\kappa^2 = 2/3$ (which implies a randomized orientation of the transition dipole moments), adenine's fluorescence yield of 6.8×10^{-5},[22] methanol's index of refraction (1.33), and the spectral overlap integral of 3.3×10^{-15} cm^6 $mmol^{-1}$,[42] the Förster radius results in a value of 5.9 Å.

Given the observed energy migration rate and the just-mentioned parameters, the "average" inter-ring distance in methanol corresponds to 8.8 Å. Whereas this distance comes from the Förster relation, it is clear that in methanol, NADH's structure is highly fluctuant.[43] As a point of reference, a molecular dynamics (MD) study of NAD^+ made in several solvents, the donor−acceptor distance in the fully unfolded state from the MD simulations in chloroform corresponds to 11.4 Å.[43] Our results about NADH's energy transfer is most likely indicative of eventual approximations of the two chromophores in this solvent.

4. CONCLUSIONS

The spontaneous emission signals of NADH were characterized through the femtosecond fluorescence up-conversion technique. After direct excitation of the dihydronicotinamide moiety with 380 nm pulses, we observed a dynamic Stokes shift of the emission band. For the methanol solutions, the time scales are similar to the reported relaxation times of this solvent. On the other hand, for NADH in aqueous solution, the red shift occurs on time scales which are at least an order of magnitude slower than the typical solvation times in water. The slower relaxation times were interpreted as because of the folded conformation of NADH in aqueous solution. That is, the shift is considered to be related to a rearrangement or structural relaxation of the folded NADH molecules after direct nicotinamidic excitation. Such relaxation includes changes in the nicotinamide-adenine contacts, which may result in changes in the interactions of the dihydronicotinamide chromophore in the excited state with its surroundings (solute−solvent and intramolecular).

We also characterized the events after 266 nm excitation. This results mainly in the local excitation of the adeninic chromophore. From a detailed study of the signals in different regions of the spectra for the model system AMP and for NADH, it was possible to consider the signals below 370 nm as being solely from the adeninic emission. From direct comparisons with the AMP signals and considering NADH's folded fraction in water, it was possible to determine that the energy transfer rate constant for the folded conformation of NADH in water corresponds to $k_{ET,folded} \approx 1.16 \times 10^{13}$ s^{-1}.

From a detailed inspection of the excitation spectrum of NADH in methanol, and the assessment of the absorption because of adenine and dihydronicotinamide at 266 nm, it was possible to determine that even in this solvent, where NADH is considered to be in an unfolded conformation, an appreciable amount of energy transfer takes place. Measurements of the fluorescence anisotropies for 266 nm excitation and 470 nm emission are consistent with the presence of a minor energy transfer channel for NADH in methanol, which accounts for approximately 43% of NADH's total emission in methanol the total yield of which upon 266 nm excitation is 3×10^{-3}. Knowledge about the typical femtosecond-resolved signals upon adenine (266 nm) excitation in NADH can serve to establish, for particular NADH-enzyme binding situations, whether this important molecule is forming an adduct with the protein as a fully unfolded state or whether its conformation remains in the folded state.[43]

■ ASSOCIATED CONTENT

Supporting Information

The Supporting Information is available free of charge at https://pubs.acs.org/doi/10.1021/acs.jpcb.9b10012.

Proton NMR spectra of NADH in aqueous and methanol solution; proton NMR chemical shift assignments for NADH in both solutions and proton NMR chemical correlations for NADH; NADH excitation spectra in different water/methanol mixtures; tables of exponential decay parameters obtained for the fluorescence decay of NADH in aqueous and methanol solutions with λ_{exc} = 266 nm and λ_{exc} = 380 nm; fluorescence anisotropy decays detected at 470 nm, exciting at 266 and 380 nm in both solvents (PDF)

■ AUTHOR INFORMATION

Corresponding Author

Jorge Peon − *Ciudad Universitaria, Ciudad de México, Mexico;* orcid.org/0000-0002-4571-5136; Email: jpeon@unam.mx

Other Authors

Andrea Cadena-Caicedo − *Ciudad Universitaria, Ciudad de México, Mexico*

Beatriz Gonzalez-Cano − *Ciudad Universitaria, Ciudad de México, Mexico*

Rafael López-Arteaga − *Ciudad Universitaria, Ciudad de México, Mexico;* orcid.org/0000-0001-8058-3469

Nuria Esturau-Escofet − *Ciudad Universitaria, Ciudad de México, Mexico;* orcid.org/0000-0002-0915-5346

Complete contact information is available at: https://pubs.acs.org/10.1021/acs.jpcb.9b10012

Notes

The authors declare no competing financial interest.

■ ACKNOWLEDGMENTS

The authors acknowledge CONACyT-Mexico grant Fronteras de la Ciencia 179 and PAPIIT/DGAPA/UNAM grant IN208618 for financial support. The authors are thankful for the NMR measurements at LURMN of UNAM's Instituto de Química.

■ REFERENCES

(1) Ghukasyan, V. V.; Heikal, A. A. *Natural Biomarkers for Cellular Metabolism: Biology, Techniques, and Applications; Series in Cellular and Clinical Imaging*; CRC Press, 2014.
(2) Formoso, E.; Mujika, J. I.; Grabowski, S. J.; Lopez, X. Aluminum and Its Effect in the Equilibrium between Folded/Unfolded Conformation of NADH. *J. Inorg. Biochem.* **2015**, *152*, 139−146.
(3) Lakowicz, J. R. *Principles of Fluorescence Spectroscopy*, 3th ed.; Springer: New York, 2006.
(4) Drozdowicz-Tomsia, K.; Anwer, A. G.; Cahill, M. A.; Madlum, K. N.; Maki, A. M.; Baker, M. S.; Goldys, E. M. Multiphoton Fluorescence Lifetime Imaging Microscopy Reveals Free-to-Bound NADH Ratio Changes Associated with Metabolic Inhibition. *J. Biomed. Opt.* **2014**, *19*, 086016.
(5) Li, D.; Zheng, W.; Qu, J. Y. Time-Resolved Spectroscopic Imaging Reveals the Fundamentals of Cellular NADH Fluorescence. *Opt. Lett.* **2008**, *33*, 2365−2367.
(6) Yu, Q.; Heikal, A. A. Two-Photon Autofluorescence Dynamics Imaging Reveals Sensitivity of Intracellular NADH Concentration and Conformation to Cell Physiology at the Single-Cell Level. *J. Photochem. Photobiol., B* **2009**, *95*, 46−57.
(7) Nakabayashi, T.; Islam, M. S.; Li, L.; Yasuda, M.; Ohta, N. Studies on External Electric Field Effects on Absorption and Fluorescence Spectra of NADH. *Chem. Phys. Lett.* **2014**, *595*−*596*, 25−30.
(8) Wang, H.-W.; Wei, Y.-H.; Guo, H.-W. Reduced Nicotinamide Adenine Dinucleotide (NADH) Fluorescence for the Detection of Cell Death. *Anti Cancer Agents Med. Chem.* **2009**, *9*, 1012−1017.
(9) Guo, H.-W.; Yu, J.-S.; Hsu, S.-H.; Wei, Y.-H.; Lee, O. K.; Dong, C.-Y.; Wang, H.-W. Correlation of NADH Fluorescence Lifetime and Oxidative Phosphorylation Metabolism in the Osteogenic Differentiation of Human Mesenchymal Stem Cell. *J. Biomed. Opt.* **2015**, *20*, 017004.
(10) Chance, B. Pyridine Nucleotide as an Indicator of the Oxygen Requirements for Energy Linked Functions of Mitochondria. *Circ. Res.* **1976**, *38*, I31.
(11) Blinova, K.; Carroll, S.; Bose, S.; Smirnov, A. V.; Harvey, J. J.; Knutson, J. R.; Balaban, R. S. Distribution of Mitochondrial NADH Fluorescence Lifetimes: Steady-State Kinetics of Matrix NADH Interactions. *Biochemistry* **2005**, *44*, 2585−2594.
(12) Hull, R. V.; Conger, P. S.; Hoobler, R. J. Conformation of NADH Studied by Fluorescence Excitation Transfer Spectroscopy. *Biophys. Chem.* **2001**, *90*, 9−16.
(13) Tropp, J.; Redfield, A. G. Proton Magnetic Resonance of NADH in Water-Methanol Mixtures. Conformational Change and Behavior of Exchangeable Proton Resonances as a Function of Temperature. *J. Am. Chem. Soc.* **1980**, *102*, 534−538.
(14) Oppenheimer, N. J.; Arnold, L. J.; Kaplan, N. O. A Structure of Pyridine Nucleotides in Solution. *Proc. Natl. Acad. Sci. U.S.A.* **1971**, *68*, 3200−3205.
(15) Couprie, M. E.; Mérola, F.; Tauc, P.; Garzella, D.; Delboulbé, A.; Hara, T.; Billardon, M. First Use of the UV Super-ACO Free-Electron Laser: Fluorescence Decays and Rotational Dynamics of the NADH Coenzyme. *Rev. Sci. Instrum.* **1994**, *65*, 1485−1495.
(16) Freed, S.; Neyfakhl, E. A.; Tumerman, L. Influence of Solvents on the Intramolecular Energy Transfer in NADH and NADPH. *Biochim. Biophys. Acta, Bioenerg.* **1697**, *143*, 432−434.
(17) Schneckenburger, H. Fluorescence Decay Kinetics and Imaging of NAD(P)H and Flavins as Metabolic Indicators. *Opt. Eng.* **1992**, *31*, 1447−1451.
(18) Blacker, T. S.; Duchen, M. R. Investigating Mitochondrial Redox State Using NADH and NADPH Autofluorescence. *Free Radic. Biol. Med.* **2016**, *100*, 53−65.
(19) Skala, M. C.; Riching, K. M.; Gendron-Fitzpatrick, A.; Eickhoff, J.; Eliceiri, K. W.; White, J. G.; Ramanujam, N. In Vivo Multiphoton Microscopy of NADH and FAD Redox States, Fluorescence Lifetimes, and Cellular Morphology in Precancerous Epithelia. *Proc. Natl. Acad. Sci. U.S.A.* **2007**, *104*, 19494−19499.
(20) Weber, G. Intramolecular Transfer of Electronic Energy in Dihydro Diphosphopyridine Nucleotide. *Nature* **1957**, *180*, 1409.
(21) Velick, S. F. Light and life. In *Structure in Enzyme Complexes of Pyridine and Flavin Nucleotides*; McElroy, W. D., Spectra, B. G., Eds.; Johns Hopkins: Baltimore, Maryland, 1971; vol. *24*, pp 55−62.
(22) Heiner, Z.; Roland, T.; Leonard, J.; Haacke, S.; Groma, G. I. Kinetics of Light-Induced Intramolecular Energy Transfer in Different Conformational States of NADH. *J. Phys. Chem. B* **2017**, *121*, 8037−8045.
(23) Villabona-Monsalve, J. P.; Noria, R.; Matsika, S.; Peón, J. On the Accessibility to Conical Intersections in Purines: Hypoxanthine and Its Singly Protonated and Deprotonated Forms. *J. Am. Chem. Soc.* **2012**, *134*, 7820−7829.
(24) Peon, J.; Zewail, A. H. DNA/RNA Nucleotides and Nucleosides: Direct Measurement of Excited-State Lifetimes by Femtosecond Fluorescence up-Conversion. *Chem. Phys. Lett.* **2001**, *348*, 255−262.
(25) Haynes, W. M. *CRC Handbook of Chemistry and Physics*; CRC Press, 2014.
(26) López-Arteaga, R.; Stephansen, A. B.; Guarin, C. A.; Sølling, T. I.; Peon, J. The Influence of Push-Pull States on the Ultrafast Intersystem Crossing in Nitroaromatics. *J. Phys. Chem. B* **2013**, *117*, 9947−9955.
(27) Arroyo-Pieck, A.; Araiza-Olivera, D.; Peon, J. Bichromophoric Sensors for Ratiometric Measurements of Molecular Microenvironments through the Interplay of Charge Transfer and Energy Transfer Channels. *ChemPlusChem* **2018**, *83*, 1097−1108.
(28) Thrippleton, M. J.; Keeler, J. Elimination of Zero-Quantum Interference in Two-Dimensional NMR Spectra. *Angew. Chem. Int. Ed.* **2003**, *42*, 3938−3941.
(29) Cohen, B.; Hare, P. M.; Kohler, B. Ultrafast Excited-State Dynamics of Adenine and Monomethylated Adenines in Solution: Implications for the Nonradiative Decay Mechanism. *J. Am. Chem. Soc.* **2003**, *125*, 13594−13601.
(30) Scott, T. G.; Spencer, R. D.; Leonard, N. J.; Weber, G. Synthetic spectroscopic models related to coenzymes and base pairs. V. Emission properties of NADH. Studies of fluorescence lifetimes and quantum efficiencies of NADH, AcPyADH, [reduced acetylpyridineadenine dinucleotide] and simplified synthetic models. *J. Am. Chem. Soc.* **1970**, *92*, 687−695.
(31) Dobek, K.; Karolczak, J.; Kubicki, J. Temperature Effects on Excitation and Deactivation Processes of Coumarin 102. A Comparison with Coumarin 153. *Dyes Pigm.* **2014**, *100*, 222−231.
(32) Gustavsson, T.; Sharonov, A.; Onidas, D.; Markovitsi, D. Adenine, Deoxyadenosine and Deoxyadenosine 5′-Monophosphate Studied by Femtosecond Fluorescence Upconversion Spectroscopy. *Chem. Phys. Lett.* **2002**, *356*, 49−54.
(33) Serrano-Andres, L.; Merchan, M.; Borin, A. C. Adenine and 2-Aminopurine: Paradigms of Modern Theoretical Photochemistry. *Proc. Natl. Acad. Sci. U.S.A.* **2006**, *103*, 8691−8696.
(34) Wu, Y.; Zheng, W.; Qu, J. Y. Sensing Cell Metabolism by Time-Resolved Autofluorescence. *Opt. Lett.* **2006**, *31*, 3122−3124.
(35) Horng, M. L.; Gardecki, J. A.; Papazyan, A.; Maroncelli, M. Subpicosecond Measurements of Polar Solvation Dynamics: Coumarin 153 Revisited. *J. Phys. Chem.* **1995**, *99*, 17311−17337.
(36) Jimenez, R.; Fleming, G. R.; Kumar, P. V.; Maroncelli, M. Femtosecond Solvation Dynamics of Water. *Nature* **1994**, *369*, 471−473.
(37) Pancur, T.; Schwalb, N. K.; Renth, F.; Temps, F. Femtosecond Fluorescence Up-Conversion Spectroscopy of Adenine and Adeno-

https://dx.doi.org/10.1021/acs.jpcb.9b10012
J. Phys. Chem. B 2020, 124, 519−530

sine: Experimental Evidence for the Πσ* State? *Chem. Phys.* **2005**, *313*, 199−212.
(38) McDonald, G.; Brown, B.; Hollis, D.; Walter, C. Some Effects of Environment on the Folding of Nicotinamide-Adenine Dinucleotides in Aqueous Solutions. *Biochemistry* **1972**, *11*, 1920−1930.
(39) Vishwasrao, H. D.; Heikal, A. A.; Kasischke, K. A.; Webb, W. W. Conformational Dependence of Intracellular NADH on Metabolic State Revealed by Associated Fluorescence Anisotropy. *J. Biol. Chem.* **2005**, *280*, 25119−25126.
(40) Zheng, W. Monitoring Changes of Cellular Metabolism and Microviscosity in Vitro Based on Time-Resolved Endogenous Fluorescence and Its Anisotropy Decay Dynamics. *J. Biomed. Opt.* **2010**, *15*, 037013.
(41) Knox, R. S. Förster's Resonance Excitation Transfer Theory: Not Just a Formula. *J. Biomed. Opt.* **2012**, *17*, 011003.
(42) Taniguchi, M.; Du, H.; Lindsey, J. S. PhotochemCAD 3: Diverse Modules for Photophysical Calculations with Multiple Spectral Databases. *Photochem. Photobiol.* **2018**, *94*, 277−289.
(43) Smith, P. E.; Tanner, J. J. Conformations of Nicotinamide Adenine Dinucleotide (NAD+) in Various Environments. *J. Mol. Recognit.* **2000**, *13*, 27−34.

https://dx.doi.org/10.1021/acs.jpcb.9b10012
J. Phys. Chem. B 2020, 124, 519−530